Case Study

# Analysis of Capture Velocity in the Case of Local Exhaust Ventilation

Szabolcs Szekeres[1]; Attila Kostyák[2]; and Imre Csáky[3]

**Abstract:** This article presents a study on the capture velocity of local exhaust ventilation (LEV) using a specially designed workstation within a laboratory setting. The workstation featured a worktop with dimensions of 90 cm width and 45 cm depth, and the exhaust duct was positioned near the pollutant source, considering the intended operation of the LEV system. The worktop was divided into squares for precise documentation and remeasurement. A supply duct above the worktop provided controlled fresh airflow. Smoke was used to visualize airflow patterns. The measurements focused on air velocity and turbulence intensity, aiming to understand flow structures and vortices. Various capture rates were tested at specific measurement points. The study revealed that the central capture lines yielded the highest efficiency. To address air extraction from behind the exhaust duct, a back sheet panel was introduced. The results showed that installing a back sheet enhanced capture velocities. The findings contribute to understanding LEV efficiency and the importance of proper design and adjustments for effective containment of contaminants in the occupational environment. **DOI: 10.1061/JAEIED.AEENG-1781**. 

**Author keywords:** Local exhaust ventilation; Air velocity; Contaminant; Workstation; Draught rate; Turbulence intensity.



## Introduction

Local exhaust ventilation (LEV) has experienced substantial integration into the manufacturing sector in recent decades. Its evolution has been driven by advancements in industry and manufacturing technology, as well as health and safety regulations. Adequate ventilation is crucial within industrial facilities, ensuring employees in occupied zones receive optimal levels of fresh air while effectively capturing and removing contaminants released during production and technological processes (ASHRAE 2003). Local exhaust systems are employed to address the localized emission of contaminants within work areas (Flynn and Susi 2012). Design engineers face complex challenges when dealing with production lines, as the technology utilized impacts the need for supply ventilation and exhaust. To prevent harmful concentrations of contaminants and pollutants in the work environment and occupied zones, either displacement ventilation and general exhaust systems are used to dilute pollutants or local exhaust ventilation is employed to capture pollutants at their source (Flynn and Susi 2012; Goodfellow and Tähti 2001). Contaminants can exist in various states and sizes, such as dust, gas, steam, mist, fume, or powder fractions, with particle sizes that can vary (Huang et al. 2016; Hayashi and Howell 1985). For effective and energy-efficient extraction and filtration of these contaminants (Duan et al. 2017), it is crucial to have precise knowledge of the amount of contaminant generated at the source within the work environment (Yang et al. 2018). Additionally, estimating the quantity of nonextracted pollutants that accumulate in the indoor air depends not only on the technology and nature of the pollutant but also on the practices of the workers using the system. Proper training of employers is necessary to accurately assess hazards and ensure safe and healthy working conditions in compliance with the Occupational Safety and Health Act (Cao et al. 2017; Whaley et al. 2021; WHO 2010). Since occupants can be negatively affected by airborne contaminants, air quality standards define permissible limits for pollutant concentrations in the workplace. LEV primarily aims to extract, separate, and filter as many contaminants as possible at the source, while general ventilation systems dilute and reduce pollutant concentrations in the premises when the extraction is imperfect. Due to the varying forms and types of contaminants, a single design for local extraction cannot cater to the needs of all areas. Moreover, the effects of pollutants on the human body differ, ranging from benign to corrosive, toxic, carcinogenic, or hazardous to health. Research explores the possibilities of extracting smoke, gas, or small-particle dust fractions released during welding or soldering operations. Welding fumes contain several particles, including chromium, which is essential to the human body (OSHA 1910) but toxic when present as industrial pollution. Various contaminants are generated during different welding processes because of diverse materials and temperatures, such as ozone, nitrogen dioxide, and nitrogen oxide, which pose significant risks at high concentrations, burdening the environment and individuals within the area. Worker exposure depends on the composition and concentration of the smoke generated. Smoke composition is influenced by the welding process, the material being welded, and the surface contamination of the workpiece. While smoke concentration primarily relies on the amount of fume generated during the welding process, posing health and safety risks to occupants (Anderson

[1]Assistant Lecturer, Faculty of Engineering, Dept. of Building Services and Building Engineering, Univ. of Debrecen, Ótemető str. 2-4, 4028 Debrecen, Hungary (corresponding author). ORCID: https://orcid.org/0000-0002-6381-869X. Email: szekeres@eng.unideb.hu

[2]Assistant Lecturer, Faculty of Engineering, Dept. of Building Services and Building Engineering, Univ. of Debrecen, Ótemető str. 2-4, 4028 Debrecen, Hungary. Email: kostyak.attila@eng.unideb.hu

[3]Associate Professor, Faculty of Engineering, Dept. of Building Services and Building Engineering, Univ. of Debrecen, Ótemető str. 2-4, 4028 Debrecen, Hungary. ORCID: https://orcid.org/0000-0001-5024-0027. Email: imrecsaky@eng.unideb.hu

Note. This manuscript was submitted on November 15, 2023; approved on January 24, 2024; published online on April 5, 2024. Discussion period open until September 5, 2024; separate discussions must be submitted for individual papers. This paper is part of the ***Journal of Architectural Engineering***, © ASCE, ISSN 1076-0431.

1997; Wanjari and Wankhede 2020). Fume generation is influenced by factors such as the type and size of the welding electrode, welding time, current, arc voltage, coatings, arc length, the air supply to the occupied zone, and the efficiency of the LEV (Marval and Tronville 2022). The use of shielding gases can also be hazardous, because gases like argon (Ar), helium (He), and carbon dioxide ($CO_2$), although not inherently toxic, displace oxygen in the air, posing risks at high concentrations, including causing headaches, nausea, dizziness, loss of consciousness, and potentially fatality (CCOHS 2023; Peelen et al. 2019). Capture efficiency assessments have been conducted for distinct operational contexts, including laboratory fume hoods, hand tool hoods, and low-volume high-velocity exhaust systems; however, a universally applicable methodology remains absent (Ellenbecker et al. 1983; Niemelä et al. 1991; Mahaki et al. 2022). Despite capture efficiency being a pivotal attribute of exhaust systems, extant studies do not scrutinize capture velocity, despite its potential to enhance overall capture efficiency when increased (Conroy et al. 1995).

## Materials and Methods

### Workstation

To facilitate the analysis of local exhaust ventilation efficiency, a specially designed workstation was constructed within a laboratory setting, allowing for repeatable measurements. The measurements were conducted at the air-ventilation and air-conditioning laboratory located at the Department of Building Services and Building Engineering, Faculty of Engineering, University of Debrecen. The workstation was strategically positioned near the pollutant source, considering the intended operation of the local exhaust system. The dimensions of the workstation's worktop are 90 cm in width and 45 cm in depth. To supply fresh air to the workstation, a supply duct was installed above the worktop, delivering a controlled airflow rate of 40 $m^3\ h^{-1}$, which corresponds to the needed fresh air rate per person for moderately heavy physical work (MSZ 21875-2, MSZ 1990). This configuration ensures a higher proportion of fresh air in the immediate head region of the person working at the workstation. To visualize the airflow patterns, smoke was introduced into the system, as depicted in Fig. 1. The workstation was placed in front of a black wall featuring a grid pattern of 600/600 mm, facilitating the visualization of airflow. A 100 mm diameter exhaust duct was centrally positioned within the workstation and the worktop, allowing for height adjustments. The worktop was divided into 15 cm squares, as illustrated in Fig. 1. The square grids serve the purpose of enabling measurements to be conducted at different points, facilitating precise documentation, and allowing for subsequent remeasurement at the same locations. This arrangement permits the comparison and analysis of measurements obtained at various capture rates within the same designated points.

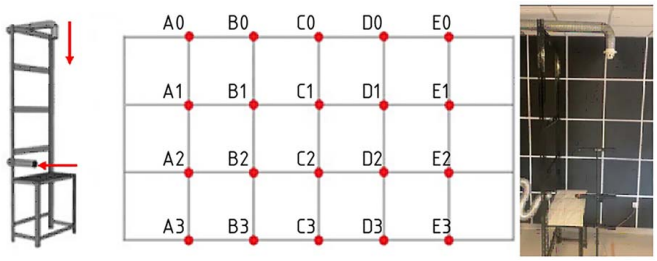


**Fig. 1.** Workstation, measurement points.

Fig. 1 reveals the formation of five horizontal lines across the width, and four vertical lines along the length. The intersection points of these lines, represented by dots and letters with Arabic numerals in Fig. 1, serve as the measurement points.

Line 0 with Measurement points A0, B0, C0, D0, and E0 is situated in alignment with the exhaust duct, occupying the same plane. Line 1 with Measurement points A1, B1, C1, D1, and E1 is positioned at a distance of 15 cm from the exhaust duct's plane, while Line 2 with Measurement points A2, B2, C2, D2, and E2 is situated 30 cm away, and Line 3 with Measurement points A3, B3, C3, D3, and E3 is 45 cm away from the plane of the exhaust duct. The exhaust duct is centrally located at Line C, resulting in Lines B and D being 15 cm apart from it, whereas Lines A and E are positioned at a distance of 30 cm from the center of the exhaust duct.

### Measuring Instruments and Methods

For conducting the measurements, calibrated instruments were employed. The prevailing air velocities at the workstation were assessed using a Testo 440 measuring instrument equipped with a turbulence intensity probe structure sensor. The calibration certificate indicates an uncertainty of 0.02 $ms^{-1}$ for the measured velocities, with a coverage factor ($k$) of 2, providing a 95% confidence level. The Testo 440 is a comprehensive air-conditioning measuring instrument featuring internal data storage and data transfer capabilities. Each measurement was obtained by averaging data collected for 3 min with a sampling frequency of 60 samples per minute. To determine the air velocity at the exhaust duct's plane, a high-precision digital vane probe with a diameter of 100 mm was employed, as depicted in Fig. 2. Visualizing the air patterns was achieved using a Martin Magnum 650 smoke machine.

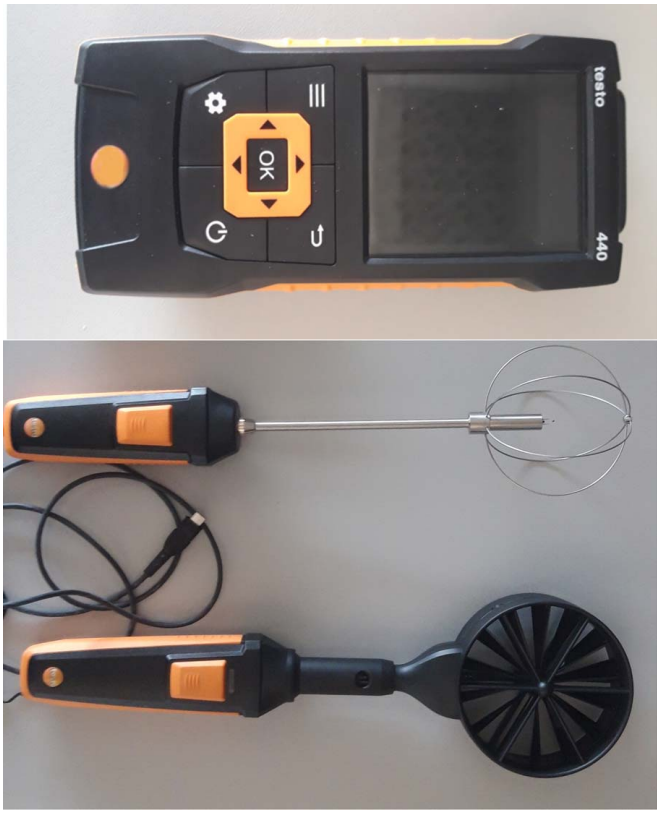


**Fig. 2.** Measuring instruments.

The measurements primarily focused on determining the mean air velocity in $ms^{-1}$ and the percentage of turbulence intensity. Turbulence measurements were conducted to explore the nature of flow structures and identify the formation of vortices within the space. These vortices can vary in size, resulting in the generation of vortices with different intensities at specific points in the flow domain, leading to fluctuations in velocity vectors. Owing to the rapid changes in the physical characteristics of air, such a flow is classified as turbulent. The level of turbulence is influenced not only by the strength of the airflow but also by the fluctuations in air velocity. Turbulence intensity was calculated using Eq. (1) per the guidelines outlined in EN ISO 7730 and EN 16798-3. Turbulence Intensity Tu (%) is obtained as follows (Szekeres et al 2022; Kalmár et al 2022):

$$Tu = \frac{\sqrt{\frac{1}{n-1} \times \sum_{i=1}^{n} (xi - \bar{x})^2}}{\bar{v}} \cdot 100\ [\%] \tag{1}$$

Initially, the capture velocity at the exhaust duct's plane was established at 4 $ms^{-1}$, followed by conducting 3-min measurements at the predetermined 20 locations. The exhaust inlet was positioned in such a way that its center was situated 5 cm from the worktop's plane. The measuring instrument was aligned with the exhaust inlet, with the sensor of the instrument positioned 5 cm from the worktop's plane. During this stage, the focus was solely on recording velocity values. The final velocity can be determined according to Eq. (2):

$$v_f = v_c \cdot \frac{5 \cdot x^2 + A}{A} \tag{2}$$

where $v_f$ = final velocity at the plane of the duct; $v_c$ = capture velocity at the plane of the measuring instrument; $x$ = distance between the measuring point and the plane of the exhaust duct; and $A$ = surface area of the exhaust duct.

The measurement value for the C0 point is absent in Fig. 3. This absence is not coincidental, as this particular point corresponds to the plane of the exhaust duct where the capture velocity was set at 4 $ms^{-1}$. The magnitude of this value is significantly higher compared with the other measured values, rendering the inclusion of these data in the diagram impractical, as it would overshadow and render the other results insignificant. Notably, the center of the exhaust inlet exhibited the highest capture rate, as anticipated, when disregarding Line 0. The presence of Line 0 indicates that suction occurs not only in the area directly in front of the nozzle but also from the sides and the rear, from where air flows into the exhaust inlet. This observation is further supported by Fig. 4, which depicts air extraction occurring from behind the extraction nozzle.

The measurements were conducted in the presence of a black-painted wall adorned with white grids, and a smoke machine was utilized to visualize the extraction process and airflow patterns surrounding the exhaust duct. This approach provided a visual representation of the dynamics occurring in the vicinity of the workstation. The observation depicted in Fig. 5 emphasizes the need to address and mitigate extraction occurring from the rear of the extraction duct. Notably, lower measured velocities were observed in Side lines A and E compared with Lines B, C, and D. As a result, these lines will be excluded from future measurements. Furthermore, it is evident that the most intense capture occurs within the first 15 centimeters, specifically in Lines 0 and 1. Consequently, two additional lines were introduced, as illustrated in Fig. 6.

These lines are measured relative to Line 0, where the first line is positioned 5 cm away, followed by a subsequent line positioned 10 cm away.

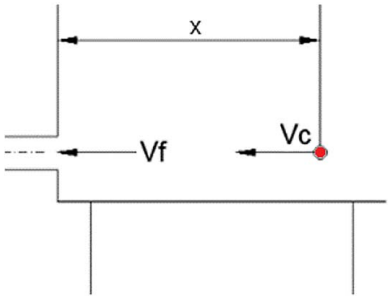


**Fig. 3.** Determination of capture and final velocity.

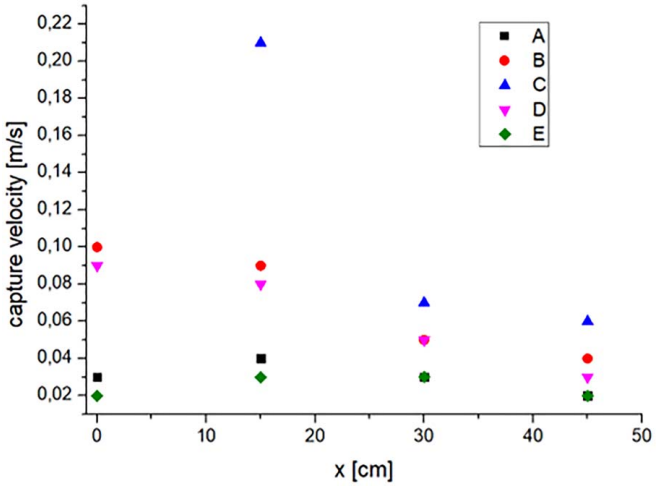


**Fig. 4.** Capture velocities at the measurement points.

**Fig. 5.** Smoke test.

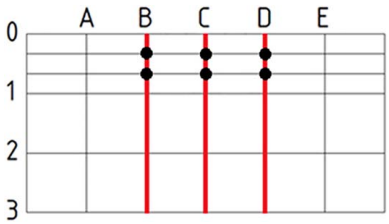


**Fig. 6.** Additional lines.

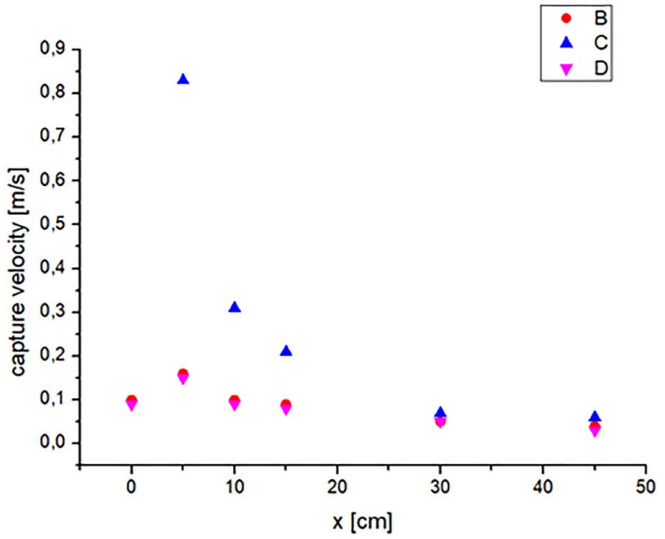


**Fig. 7.** Capture velocities at the measurement points with the additional lines.

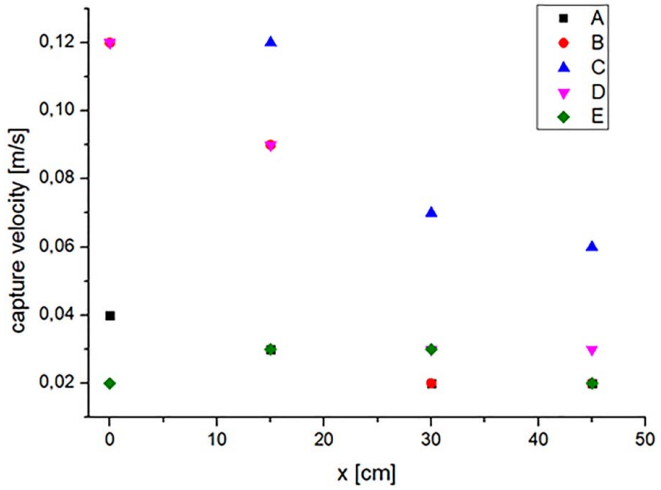


**Fig. 8.** Capture velocities at the measurement points with the extraction nozzle at 10 cm from the plane of the worktop.

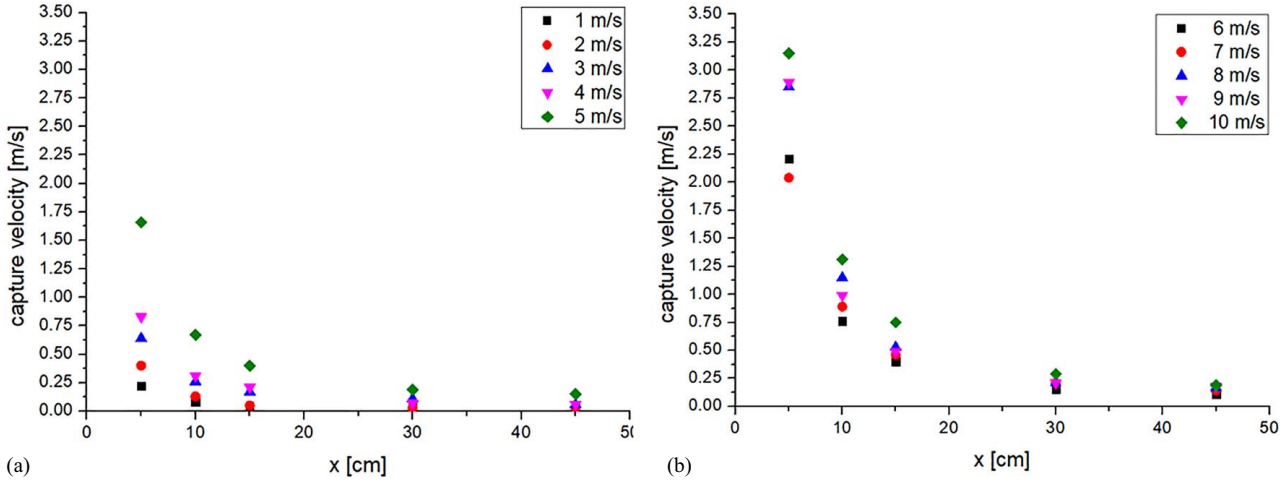


**Fig. 9.** Capture velocities at the measurement points. The capture velocity at the plane of the exhaust duct was set between (a) 1–5 $ms^{-1}$; and (b) 6–10 $ms^{-1}$.

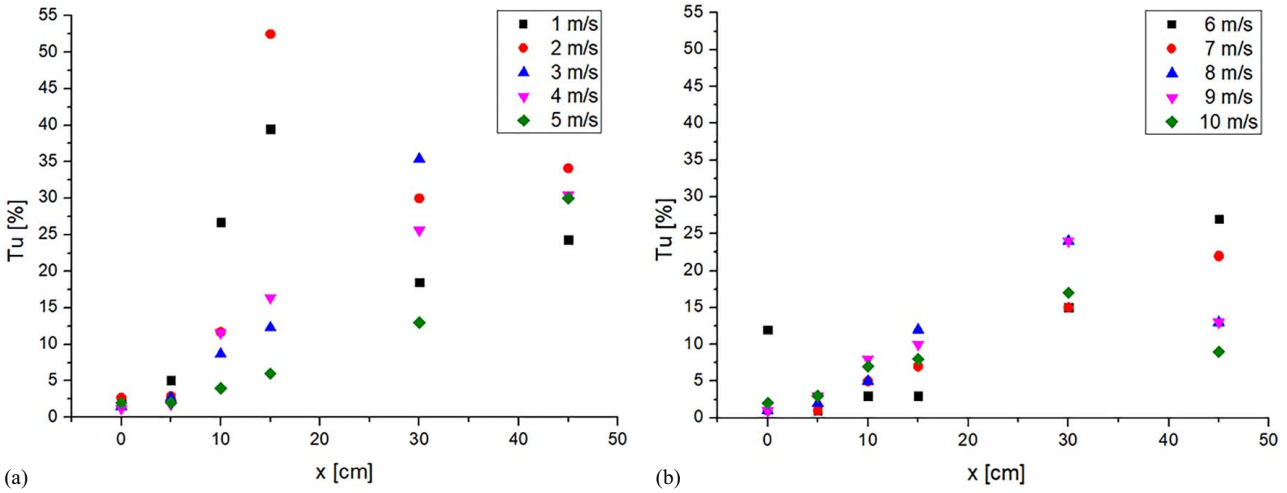


**Fig. 10.** Turbulence intensity at the measurement points. The capture velocity at the plane of the exhaust duct was set between (a) 1–5 $ms^{-1}$; and (b) 6–10 $ms^{-1}$.

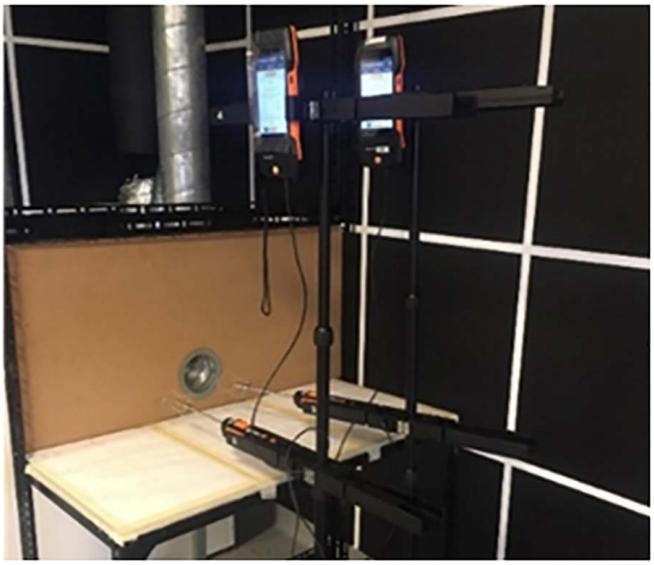

**Fig. 11.** Workstation with back sheet panel.

### *Measurement Results with the Additional Measuring Points*

Consequently, a new set of measurements was conducted exclusively in Lines B, C, and D, resulting in the creation of six additional measurement points as depicted in Fig. 6.

Conducting additional measurements at the central region of the extraction nozzle is of significance, given its higher capture rate throughout the entire depth of the workstation. In the subsequent series of measurements, the exhaust velocity of the extraction remained constant, with the sole modification being the repositioning of the suction nozzle. Specifically, the nozzle was elevated so that its centerline was positioned 10 cm from the worktop's plane. The measuring instrument was adjusted to this height, and the measurements were carried out at the predetermined points established previously Fig. 7.

The preceding series of measurements reveals that the proximity of the worktop to both the measuring instrument and the extraction nozzle influences the capture rate. Specifically, in Lines B, C, and D, the capture rate demonstrates the highest significance, warranting further investigation at these points while temporarily disregarding the remaining ones. The previous measurements have consistently

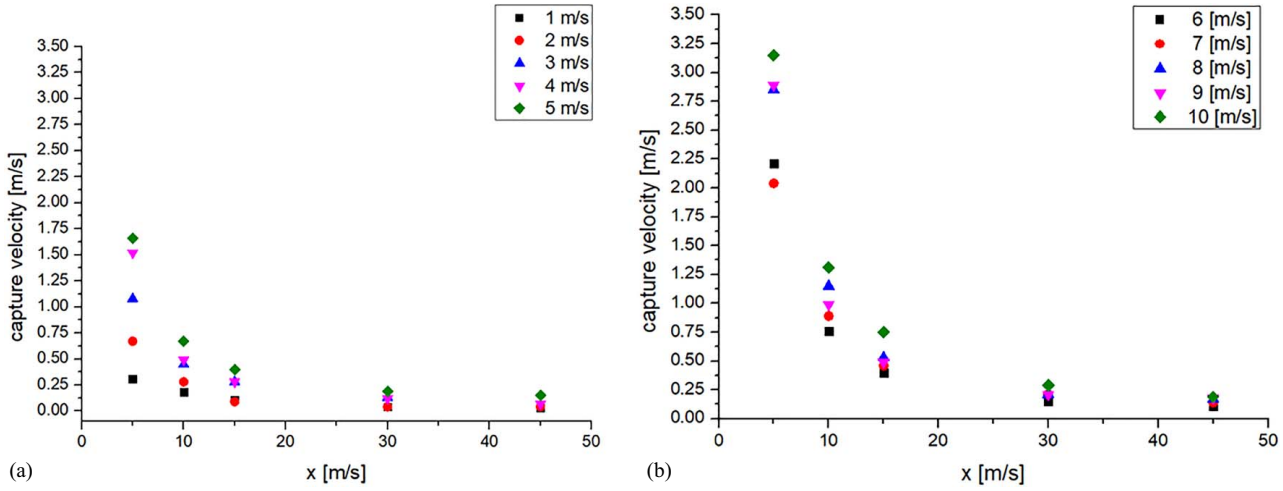


**Fig. 12.** Capture velocities at the measurement points. The capture velocity at the plane of the exhaust duct was set between (a) 1–5 $ms^{-1}$; and (b) 6–10 $ms^{-1}$.

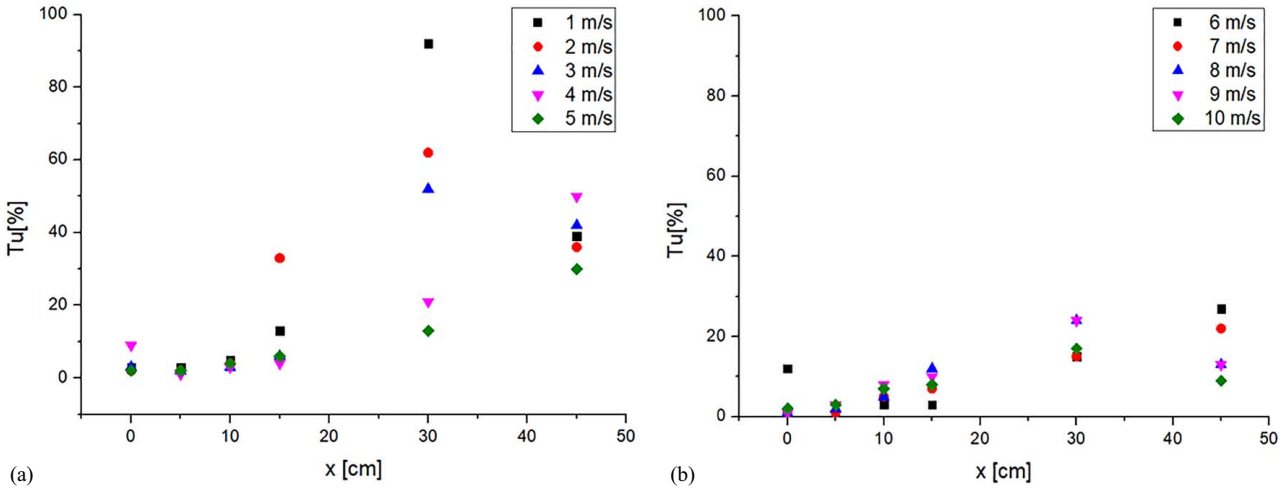


**Fig. 13.** Turbulence intensity at the measurement points. The capture velocity at the plane of the exhaust duct was set between (a) 1–5 $ms^{-1}$; and (b) 6–10 $ms^{-1}$.

**Table 1.** Capture velocity averages

| Average velocity | Without back sheet | With back sheet |
|---|---|---|
| 1 $ms^{-1}$ $\bar{v}$ | 0.235 | 0.278 |
| 2 $ms^{-1}$ $\bar{v}$ | 0.44 | 0.52 |
| 3 $ms^{-1}$ $\bar{v}$ | 0.71 | 0.84 |
| 4 $ms^{-1}$ $\bar{v}$ | 0.91 | 1.08 |
| 5 $ms^{-1}$ $\bar{v}$ | 1.14 | 1.35 |
| 6 $ms^{-1}$ $\bar{v}$ | 1.358 | 1.605 |
| 7 $ms^{-1}$ $\bar{v}$ | 1.56 | 1.85 |
| 8 $ms^{-1}$ $\bar{v}$ | 1.82 | 2.15 |
| 9 $ms^{-1}$ $\bar{v}$ | 1.94 | 2.29 |
| 10 $ms^{-1}$ $\bar{v}$ | 2.21 | 2.62 |

shown that the central capture lines yield the highest results. Hence, it is imperative to conduct additional measurements along the centerline, covering a range of capture velocities from 1 to 10 $ms^{-1}$.

### Measurements in Line C of the Workstation

Apart from the velocity, the turbulence intensity is determined as well.

Fig. 9 illustrates that the capture velocities, with an initial velocity range of 1–3 $ms^{-1}$ at the extraction nozzle plane, exhibit negligibly low values, particularly at distances of 10 cm or greater.

Figs. 8 and 9 clearly demonstrate that as the distance from the exhaust duct increases, the measured velocities at the designated points experience a significant decline at lower extraction velocities, while the turbulence intensity intensifies. To address the observed phenomenon illustrated in Fig. 4, where the exhaust duct captures air from behind, a back sheet panel was installed on the workstation in the subsequent round of measurements. By introducing the back sheet panel, it is anticipated that the capture velocity at the measurement points would surpass that of the previous measurement set. The measurements were exclusively conducted in Line C, as the preceding series of measurements confirmed its superior efficiency. This allows for a comparison of results obtained without and with the back sheet panel, providing valuable insights into the impact of its installation Fig. 10.

### Measurements in Line C with Back Sheet Panel

As can be seen in Fig. 11, a back sheet panel was mounted around the exhaust duct (Fig. 12).

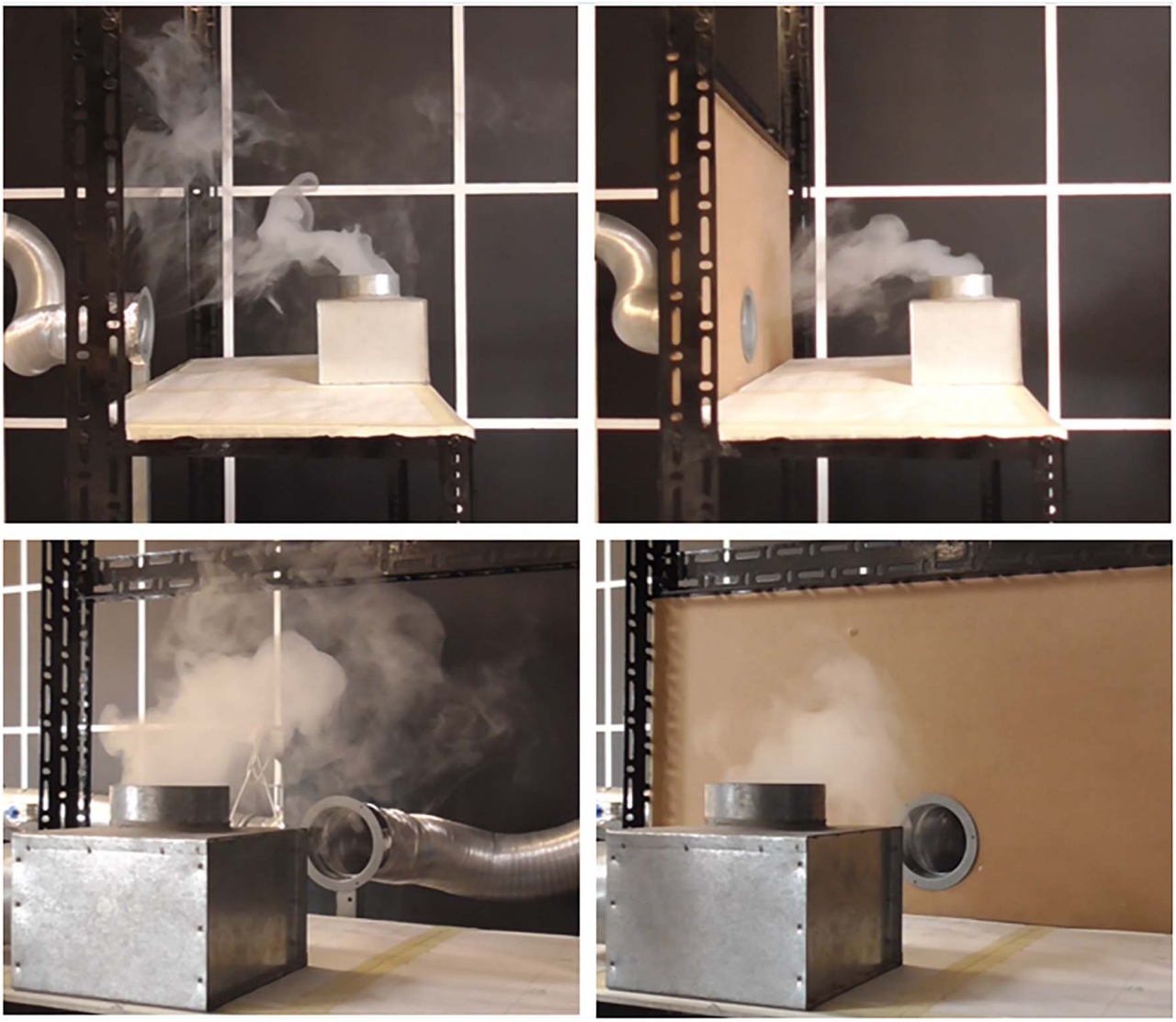

**Fig. 14.** Smoke test with the back sheet panel.

Fig. 13 provides evidence that the zone located beyond a 10 cm distance from the extraction point exhibits a considerably higher degree of flow turbulence, particularly at lower velocities. Consequently, relying solely on the calculated capture velocity determined by Eq. (2) is inadequate when the workplace and contaminant discharge are more distanced. In the case of a steady flow over time, the turbulence degree remains at 0%, signifying an unchanging capture velocity at the specific measurement point. Conversely, elevated turbulence intensity leads to significant deviations from the designated capture velocity at various instances. When a negative deviation from the average rate is observed, it indicates an insufficient capture rate for removing the contaminant from the occupied zone. Based on the aforementioned observations, it can be concluded that augmenting the set velocity at the exhaust nozzle such that it maintains low turbulence intensity is likely to establish an appropriate capture velocity at the contaminant source. In our specific scenario, this implies applying safety factors of 1.1 and 1.4 for work conducted 30–45 cm away from the extraction point, respectively, to ensure effective containment of the contaminant. Such an approach necessitates a significant increase in the extraction volume flow. To visually assess the efficiency of the workstation extraction, smoke was introduced into a junction box, simulating a workpiece on the workstation worktop. This allows for the observation of smoke movement toward the exhaust inlet from a position higher than the centerline of the opening, as depicted in Fig. 14.

Fig. 14 effectively represents the measurement outcomes. The images clearly illustrate that in the absence of a back cover, the smoke rises to significantly greater heights. This observation substantiates the need for a higher capture rate when operating without a back sheet to prevent contaminants from entering the occupied zone of a seated individual at a height of 1.1 m or a standing individual at a height of 1.7 m, as prescribed by standards.

Introducing a back sheet enhances the efficiency of the extraction system. However, prior to installing a back sheet on the workstation, careful consideration must be given to the size of the workpieces being handled on the worktop. The workpiece should be smaller than the surface area of the worktop, as the presence of a backing may pose an obstacle and restrict work on larger workpieces.

To analyze the results of the two-measurement series, the capture rates at the measurement points were averaged. The percentage difference between the average velocities (DAV) in the case of the two exhaust modes was calculated using Eq. (3). The average velocities, denoted as the average velocities measured at the five measurement points, are determined as follows:

$$\mathrm{DAV} = \frac{\text{avarage 2}}{\text{avarage 1}} \cdot 100\ [\%] \tag{3}$$

The term *average 2* represents the average of the capture rates obtained when the back sheet was used, while *average 1* signifies the average of the capture rates measured in the absence of the back sheet. Table 1 depicts the average velocities measured under both conditions, with and without the back sheet.

## Discussion and Conclusions

This article presents a study conducted on the capture velocity of local exhaust ventilation, specifically focusing on the impact of a back sheet installed on a workbench to enhance capture velocities. The investigation aims to examine the differences in average capture velocity at six measurement points when using the back sheet compared with its absence, which ranges from 18% to 18.6%.

Turbulence intensity plays a crucial role in influencing the capture velocity. When turbulence intensity is high, the capture velocity may deviate significantly from the required set velocity at certain moments. To address this, it is necessary to introduce a multiplicative factor to the set values to always ensure an appropriate exhaust level and capture velocity. However, caution must be exercised when adjusting this factor. For example, setting a 10% increase to a 4 $ms^{-1}$ set velocity at the exhaust duct results in an excess air volume of 11 $m^3\ h^{-1}$, whereas at 10 $ms^{-1}$, it increases to 28 $m^3\ h^{-1}$. Similarly, a 20% increase at 4 $ms^{-1}$ yields an excess air volume of 23 $m^3\ h^{-1}$, while at 10 $ms^{-1}$, it rises to 56 $m^3\ h^{-1}$. It is important to consider the impact on the general ventilation system, as it will need to supply the exhausted air. The lower the set flow rate, the lower the ventilation work as well.

Based on the measurement results presented, it is evident that compared with empirical formulas determining extraction capture velocity, a multiplicative factor ranging from 1.1 to 1.4 must be applied to achieve optimal exhaust performance.

If we can mount a back panel to our workstation, we can provide more effective extraction. The velocity set in the free cross section of the exhaust duct can even be reduced, thereby saving ventilation work and energy. As shown in Fig. 14, the contaminants released at the workstation do not reach the breathing zone of the person working there when a back panel is used, therefore preventing the inhalation of polluted air. Because fresh air is also supplied at the top of the workstation, a continuous supply of fresh air envelops the worker that also prevents inhalation of polluted air.

## Future Work

Given that the measurements conducted thus far were limited to a Ø100 mm diameter duct, there is a need to extend the scope of the measurements and conduct further analysis. The objective would be to assess whether modifying the dimensions of the extraction duct results in a consistent and comparable variation in average velocities, both in the presence and absence of a back sheet. Additionally, an energy study of the fan power consumption at various flow rates and the exhaust system should be undertaken to evaluate its efficiency and performance.

## Data Availability Statement

Some or all data, models, or codes that support the findings of this study are available from the corresponding author upon reasonable request.

## Acknowledgments

Project no. TKP2021-NKTA-34 has been implemented with the support provided by the Ministry of Innovation and Technology of Hungary from the National Research, Development, and Innovation Fund, financed under the TKP2021-NKTA funding scheme.

Author contributions: S.S. and A.K.: Conceptualization, methodology, software, validation, formal analysis, investigation, recourses, data curation, writing—original draft preparation; writing—review and editing; visualization; supervision; and funding acquisition. I.C.: Conceptualization, methodology, software, validation, formal analysis, investigation, recourses, data curation, writing—original draft preparation; writing—review and editing; visualization; supervision; project administration; and funding acquisition.

## References


Anderson, R. A. 1997. "Chromium as an essential nutrient for humans." *Regul. Toxicol. Pharm.* 26: S35–S41. https://doi.org/10.1006/rtph.1997.1136.

ASHRAE (American Society of Heating, Refrigerating and Air-Conditioning Engineers). 2003. *ASHRAE handbook, HVAC Applications, Chapter 29 Ventilation of the industrial environment, Chapter 30 Industrial local exhaust systems*. Peachtree Corners, GA: ASHRAE.

Cao, Z., Y. Wang, M. Duan, and H. Zhu. 2017. "Study of the vortex principle for improving the efficiency of an exhaust ventilation system." *Energy Build.* 142: 39–48. https://doi.org/10.1016/j.enbuild.2017.03.007.

CCOHS (Canadian Centre for Occupational Health and Safety). 2023. Accessed January 23, 2023. https://www.ccohs.ca/oshanswers/safety_haz/welding/fumes.html#:~:text=Welding%20fumes%20are%20a%20complex,and%20the%20material%20being%20welded.

Conroy, L. M., R. S. Prodans, M. Lachman, X. Yu, R. A. Wadden, J. E. Franke, and P. A. Scheff. 1995. "Hood efficiencies of vapor degreasers under operating conditions." *J. Environ. Eng.* 121 (10): 736–741. https://doi.org/10.1061/(ASCE)0733-9372(1995)121:10(736).

Duan, M., Y. Wang, D. Gao, Y. Yang, and Z. Cao. 2017. "Modeling dispersion mode of high-temperature particles transiently produced from industrial processes." *Build. Environ.* 126: 457–470. https://doi.org/10.1016/j.buildenv.2017.10.016.

Ellenbecker, M. J., R. F. Gempel, and W. A. Burgess. 1983. "Capture efficiency of local exhaust ventilation systems." *Am. Ind. Hyg. Assoc. J.* 44 (10): 752–755. https://doi.org/ 10.1080/15298668391405689.

Flynn, M. R., and P. Susi. 2012. "Local exhaust ventilation for the control of welding fumes in the construction industry—A literature review." *Ann. Occup. Hyg.* 56 (7): 764–776. https://doi.org/10.1093/annhyg/mes018.

Goodfellow, H., and E. Tähti. 2001. *Industrial ventilation design guidebook*. Cambridge, MA: Academic Press—A Harcourt Science and Technology Company.

Hayashi, T., and R. H. Howell. 1985. *Industrial ventilation and air conditioning*. Washington, DC: Office of Scientific and Technical Information (OSTI).

Huang, Y., Y. Wang, X. Ren, Y. Yang, J. Gao, and Y. Zou. 2016. "Ventilation guidelines for controlling smoke, dust, droplets and waste heat: Four representative case studies in Chinese industrial buildings." *Energy Build.* 128: 834–844. https://doi.org/10.1016/j.enbuild.2016.07.046.

Kalmár, T., F. Szodrai, and F. Kalmár. 2022. "Experimental study of local effectiveness in the case of balanced mechanical ventilation in small offices." *Energy* 244 (Part A): 122619. https://doi.org/10.1016/j.energy.2021.122619.

Mahaki, M., M. Mattsson, M. Salmanzadeh, and A. Hayati. 2022. "Experimental and numerical simulations of human movement effect on the capture efficiency of a local exhaust ventilation system." *J. Build. Eng.* 52: 104444. https://doi.org/10.1016/j.jobe.2022.104444.

Marval, J., and P. Tronville. 2022. "Ultrafine particles: A review about their health effects, presence, generation, and measurement in indoor environments." *Build. Environ.* 216: 108992. https://doi.org/10.1016/j.buildenv.2022.108992.

MSZ. 1990. "Labour safety requirements of heating and ventilation of workplaces." *Elimination of the contaminations from workplace air*. 21875-2:1990. Budapest, Hungary: Hungarian Standards Institution.

Niemelä, R., A. Lefevre, J. P. Muller, and G. Aubertin. 1991. "Comparison of three tracer gases for determining ventilation effectiveness and capture efficiency." *Ann. Occup. Hyg.* 35 (4): 405–417. https://doi.org/10.1093/annhyg/35.4.405.

OSHA (Occupational Safety and Health Administration). 1910. "Hazard communication." Accessed November 20, 2023. https://www.osha.gov/laws-regs/regulations/standard\ number/1910/1910.1200.

Peelen, R. V., B. P. Ramakers, and A. Koopmans. 2019. "The dangers of argon, an inert industrial gas: Beware of asphyxiation." *Neth. J. Crit. Care* 27 (4).

Szekeres, S., A. Kostyák, F. Szodrai, and I. Csáky. 2022. "Investigation of ventilation systems to improve air quality in the occupied zone in office buildings." *Buildings* 12 (4): 493. https://doi.org/10.3390/buildings12040493.

Wanjari, M. B., and P. Wankhede. 2020. "Occupational hazards associated with welding work that influence health status of welders." *Int. J. Curr. Res. Rev.* 12 (23): 51–55. https://doi.org/10.31782/IJCRR.2020.122303.

Whaley, P., M. Nieuwenhuijsen, and J. Burns. 2021. "Update of the WHO global air quality guidelines: systematic reviews." *Environment International 142(Special issue)*. Accessed January 23, 2023. https://www.sciencedirect.com/journal/environment-international/special-issue/10MTC4W8FXJ.

WHO (World Health Organization). 2010. "WHO guidelines for indoor air quality: Selected pollutants." *World Health Organization. Regional Office for Europe*. Geneva, Switzerland: WHO.

Yang, Y., Y. Wang, B. Song, J. Fan, and Y. Cao. 2018. "Stability and accuracy of numerical investigation of droplet motion under local ventilation airflow." *Build. Environ.* 140: 32–42. https://doi.org/10.1016/j.buildenv.2018.05.023.